Molecular Biology of the Cell
Vol. 18, 337–347, February 2007

Internalization of Large Double-Membrane Intercellular Vesicles by a Clathrin-dependent Endocytic Process[V]

Michelle Piehl,*† Corinna Lehmann,*†‡ Anna Gumpert,* Jean-Pierre Denizot,§ Dominique Segretain,‖ and Matthias M. Falk*

*Department of Biological Sciences, Lehigh University, Bethlehem, PA 18015; §Unité de Neurosciences Intégratives et Computationnelles, Centre National de la Recherche Scientifique UPR 2191, Gif sur Yvette 91198 Cedex, France; and ‖Institut National de la Santé et de la Recherche Médicale U670, Université de Paris 5, Paris, France

Submitted June 5, 2006; Revised October 19, 2006; Accepted November 2, 2006
Monitoring Editor: Asma Nusrat

Beyond its well-documented role in vesicle endocytosis, clathrin has also been implicated in the internalization of large particles such as viruses, pathogenic bacteria, and even latex beads. We have discovered an additional clathrin-dependent endocytic process that results in the internalization of large, double-membrane vesicles at lateral membranes of cells that are coupled by gap junctions (GJs). GJ channels bridge apposing cell membranes to mediate the direct transfer of electrical currents and signaling molecules from cell to cell. Here, we report that entire GJ plaques, clusters of GJ channels, can be internalized to form large, double-membrane vesicles previously termed annular gap junctions (AGJs). These internalized AGJ vesicles subdivide into smaller vesicles that are degraded by endo/lysosomal pathways. Mechanistic analyses revealed that clathrin-dependent endocytosis machinery-components, including clathrin itself, the alternative clathrin-adaptor Dab2, dynamin, myosin-VI, and actin are involved in the internalization, inward movement, and degradation of these large, intercellular double-membrane vesicles. These findings contribute to the understanding of clathrin's numerous emerging functions.

INTRODUCTION

The role of clathrin in endocytosis is well documented. This protein forms a typical curved lattice around endocytic vesicles that are internalized at the plasma membrane (PM). In addition, the involvement of clathrin in several uncharacteristic endocytic processes has been reported, including the internalization of viruses, pathogenic bacteria, and large latex beads (Aggeler and Werb, 1982; Ehrlich *et al*., 2004; Rust *et al*., 2004; Veiga and Cossart, 2005). Here, we describe another function of the clathrin-dependent endocytic machinery that results in the internalization of large, double-membrane vesicles at lateral PMs of cells that are coupled by gap junctions (GJs).

GJs are ubiquitously distributed channels that connect the cytoplasms of two apposing cells each participating in this connection via a half channel termed a connexon to provide direct cell-to-cell communication. Connexons are hexamers of four-pass membrane proteins called connexins (Cxs; Bruzzone *et al*., 1996; Kumar and Gilula, 1996). Once transported to the PM, GJ channels cluster into two-dimensional arrays termed plaques that can be composed of a few to many thousands of individual channels and vary from a few square nanometers to many square micrometers (Bruzzone *et al*., 1996; Falk, 2000a; Severs *et al*., 2001). GJ channels can open and close (gate) and physiological parameters, including intracellular pH, Ca^{2+} concentration, and Cx phosphorylation, are known to modulate GJ channel gating and the extent of GJ-mediated intercellular coupling (Delmar *et al*., 2004; Lampe and Lau, 2004; Moreno, 2005). However, the extent of intercellular coupling could also be regulated through altering the number of GJ channels in the PM.

Cxs have a surprisingly short half-life of only 1–5 h, leading to a rapid GJ and Cx protein turnover (Fallon and Goodenough, 1981; Beardslee *et al*., 1998; Berthoud *et al*., 2004). Additional studies have shown that docked connexons cannot be separated under physiological conditions (Goodenough and Gilula, 1974; Ghoshroy *et al*., 1995), suggesting that GJ degradation could occur via the internalization of complete double-membrane spanning GJ plaques. Structural and ultrastructural analyses of differentiating tissues and cells in culture have shown cytoplasmically located, double-membrane GJ vesicles that were termed annular gap junctions (AGJs; Ginzberg and Gilula, 1979; Larsen *et al*., 1979; Leach and Oliphant, 1984; Mazet *et al*., 1985; Jordan *et al*., 2001), leading to the hypothesis that AGJ vesicles represent internalized GJs.

To test this hypothesis, we investigated the spatiotemporal process of GJ degradation in living and fixed HeLa cells that transiently or stably expressed fluorescent protein-tagged Cx43 (Cx43-green fluorescent protein [GFP], -cyan fluorescent protein [CFP], and -yellow fluorescent protein [YFP]). We then examined these cells by time-lapse fluorescence microscopy combined with ultrastructural analyses.

This article was published online ahead of print in *MBC in Press* (http://www.molbiolcell.org/cgi/doi/10.1091/mbc.E06–06–0487) on November 15, 2006.

[V] The online version of this article contains supplemental material at *MBC Online* (http://www.molbiolcell.org).

† These authors contributed equally to this work.

‡ Present address: Olympus Deutschland GmbH, Wendenstrasse 16-18, Hamburg, Germany.

Address correspondence to: Matthias M. Falk (mfalk@lehigh.edu).

Our studies demonstrate for the first time that entire GJ plaques can internalize to form large intracellular GJ vesicles. These vesicles are then fragmented into smaller vesicles that are degraded by endo/lysosomal pathways. To understand the mechanism of GJ internalization, the role of a number of proteins known to play a critical role in endocytosis was investigated. Our results show that proteins critical for clathrin-dependent endocytosis, including the coat protein clathrin itself, the alternative clathrin-adaptor Dab2, dynamin, myosin-VI, and actin filaments are used to internalize, translocate, and degrade double-membrane spanning GJ channel plaques. Depleting cells of clathrin by RNA interference (RNAi), and expressing Cx43-GFP in cells that express only low amounts of Dab2 (COS-7) demonstrated that interaction and recruitment of both proteins is highly specific and that clathrin depletion significantly reduces GJ internalization. To our knowledge, this report is the first to describe that a combination of proteins including clathrin, Dab2, dynamin, and myosin-VI can be used to internalize and translocate large double-membrane vesicles.

MATERIALS AND METHODS

cDNA Constructs

Fluorescent protein-tagged Cx43 constructs were described previously (Falk, 2000). The GFP-tagged myosin-VI full-length construct (GFP-M6full, generously provided by T. Hasson, University of California, San Diego, La Jolla, CA) was described previously (Aschenbrenner *et al*., 2003). Localization of phosphatidylinositol-4,5-bisphosphate [PtdIns(4,5)P_2] to GJ plaques was examined by expressing the pleckstrin homology (PH) domain of phospholipase C_δ fused to GFP (generously provided by L. Traub, University of Pittsburgh, Pittsburgh, PA) as described previously (Varnai and Balla, 1998) combined with immunofluorescent detection of Cx43.

Antibodies and Staining Reagents

Goat anti-clathrin heavy chain antibodies (Sigma-Aldrich, St. Louis, MO), anti-clathrin heavy chain monoclonal antibodies (mAbs) clone 23 (BD Biosciences, San Jose, CA), X22 (Chin *et al*., 1989), and rabbit polyclonal clathrin light-chain antibody 4878 (generously provided by S. Schmid, The Scripps Research Institute, La Jolla, CA) were used at dilutions of 1:100–1:250. Anti-α-adaptin (AP-2 subunit) mAbs (clone AP6; Affinity Bioreagents, Golden, CO) were used at a dilution of 1:200. Anti-Dab-2/p96 (clone52; BD Biosciences) and anti-myosin-VI tail mAbs, generously provided by T. Hasson (University of California, San Diego; Hasson and Mooseker, 1994), were used at 1:50 and 1:100 dilutions, respectively. Human nonmuscle myosin-IIA and -IIB heavy chain-specific rabbit anti-peptide antibodies (BAbCO, Richmond, CA) were used at 1:200 dilutions. Polyclonal rabbit anti-epsin 1 and monoclonal anti-CALM antibodies (generously provided by L. Traub) were used at 1:500 and 1:100 dilutions, respectively. Anti-dynamin mAbs (clone 41; BD Biosciences) were used at 1:250 dilutions. Rabbit polyclonal anti-Cx43 antibodies (Zymed Laboratories, South San Francisco, CA) were used at a dilution of 1:200. Secondary antibodies conjugated to Cy3, Texas Red, or Alexa Fluor (Jackson ImmunoResearch Laboratories, West Grove, PA and Invitrogen, Carlsbad, CA), respectively, were used at 1:100–1:200 dilutions. The membrane stain DiI (Invitrogen) was added to growth medium at concentrations of 5 μM for 2 min, followed by medium exchange and immediate observation. A quantum dot solution (Qtracker 655; Invitrogen) was microinjected at a needle concentration of 400 nM in injection buffer as described previously (Piehl and Cassimeris, 2003). A rhodamine-phalloidin stock solution was prepared according to manufacturers directions (Invitrogen) and used at a dilution of 1:200 in PBS for 10 min.

Cell Culture, Stable and Transient Transfections, and Immunofluorescence Labeling

Human epitheloid cervix carcinoma cells (HeLa, ATCC CCL 2; American Type Culture Collection, Manassas, VA) and African green monkey kidney cells (COS-7, ATCC CRL 1650; American Type Culture Collection) were maintained under standard conditions as described previously (Falk, 2000). Inducible, stable transfected HeLa tet-on cell lines expressing Cx43-CFP, and Cx43-YFP, respectively, were constructed and induced as described previously (Lauf *et al*., 2002). For transfections, inductions, and stainings, cells were seeded on 22-mm round cover glasses placed in 35-mm cell culture dishes and grown to ~70% confluence. The following day, appropriate cells were transfected with Superfect transfection reagent (QIAGEN, Valencia, CA) as described by the manufacturer. Twenty-four hours later, cells were fixed and permeabilized either with methanol, or 2% formaldehyde for 10 min, washed three times in phosphate-buffered saline (PBS) (between all steps), followed by incubations for 30 min in 0.1% Triton X-100, and 2% bovine serum albumin (BSA)/PBS blocking solution. Cells were incubated with antibodies for 1 h at room temperature, rinsed in PBS, and mounted with Fluoromount G (Southern Biotechnology Associates, Birmingham, AL).

Fluorescence Microscopy

Time-lapse microscopy was performed on a Nikon Eclipse TE 2000E inverted fluorescence microscope equipped with 40× Plan Fluor (numerical aperture [NA]1.3), 60× and 100× Plan Apochromat (NA1.4) oil immersion lenses; a forced-air-cooled Photometics CoolSnap HQ charge-coupled device camera (Roper Scientific, Duluth, GA) and a ProScan II motorized stage (Prior Scientific, Rockland, MA). Cells were grown on round, 30-mm-diameter coverslips and mounted in a closed-exchange POC Mini live cell chamber (PeCon, Erbach, Germany). Openings were connected to a 5% CO_2 gassed medium reservoir on one side, and a microperfusion pump (Instech Laboratories, Plymouth Meeting, PA) (flow rate 300 μl/h) on the other side. The interior of a custom-made Plexiglas incubator encasting the entire microscope system was heated to 37°C. Images were captured, analyzed, and processed using MetaVue software version 6.1r5 (Molecular Devices, Sunnyvale, CA) and Adobe Photoshop (Adobe Systems, Mountain View, CA). Fluorescence colocalization analyses were performed on a Zeiss Axiovert 200 M inverted fluorescence microscope (Carl Zeiss, Jena, Germany) equipped with an LSM510 META scan head and a 63× Apochromat oil-immersion lens (NA1.4). Argon ion and HeNe lasers were used to generate the 488- and 543-nm excitation lines, and pinholes were typically set to 1 airy unit. Images were acquired using two-line mean averaging in separated channels to avoid bleed through and LSM510 META 3.0 software. Deconvolution microscopy was performed as described previously (Falk, 2000).

Ultrastructural Analyses

HeLa cells were transiently transfected with GFP-tagged Cx43 and incubated overnight. Cells were fixed in 3.5% glutaraldehyde in 1× PBS for 1 h at room temperature (RT). After an overnight rinse in 1× PBS cells were postfixed in 1% osmium tetroxyde (1 h at RT). Cells were dehydrated in an ethanol series and flat embedded in Epon. Embedded cells were mounted and thin-sectioned using an LKB Ultotome NOVA ultramicrotome (GE Healthcare, Little Chalfont, Buckinghamshire, United Kingdom). Thin sections were stained with uranyl acetate and lead citrate and examined with a Phillips CM10 electron microscope.

Drug Treatments

Actin filaments were stabilized or disrupted by treating cells with jasplakinolide (Calbiochem, San Diego, CA; 0.5 μM, stock in dimethyl sulfoxide [DMSO]), cytochalasin D (Sigma-Aldrich; 0.3 μM, stock in DMSO), or latrunculin A (Sigma-Aldrich; 1 μM, stock in DMSO) for 1 h. AGJ dynamics were tracked from time-lapse image sequences (typically 2- to 3-min intervals) by using the "Track Objects" application of MetaMorph (Molecular Devices). Clathrin-dependent endocytosis was inhibited by treating cells with hypertonic medium (0.2 M sucrose) for 3 h as described previously (Hansen *et al*., 1993). Myosin-II was inhibited by treating cells with 100 μM blebbistatin (Calbiochem; stock in DMSO) for 4 h.

RNAi Assays

Two double-stranded RNA oligonucleotides (oligos) corresponding to clathrin heavy chain (#1 sense [s]: 5′-AUCCAAUUCGAAGACCAAUTT-3′; antisense [as]: 5′-AUUGGUCUUCGAAUUGGAUTT-3′; #2 [s]: 5′-CCUGCGGUCUGGAGUCAACTT-3′; [as]: 5′-GUUGACUCCAGACCGCAGGTT-3′) and fluorescently labeled control RNA (siGLO RISC-free fluorescently labeled, nontargeting oligo) were purchased from Dharmacon RNA Technologies (Lafayette, CO) and transfected into HeLa cells using Oligofectamine (Invitrogen), followed 48 h later by Cx43-GFP cDNA using Superfect (QIAGEN) as recommended by the manufacturers. Cells were assayed 72 h after oligo transfection. Efficiency of clathrin-dependent endocytosis inhibition was monitored by incubation in medium containing 10 μg/ml Alexa Fluor 488-labeled transferrin (5 mg stock solution in 1× PBS; Molecular Probes) for 3 min, fixation, and microscopic examination.

Immunoblot Analyses

Total cell lysates were separated on 6–8% acrylamide mini-gels (Bio-Rad, Hercules, CA), transferred onto nitrocellulose membranes, and blocked with 5% dry milk. Membranes were incubated in polyclonal anti-Dab2 (generously provided by L. Traub; 1:5000 dilution), anti-clathrin heavy chain (monoclonal CHC 610499; BD Biosciences), and monoclonal anti-β-tubulin (clone E7; Developmental Studies Hybridoma Bank, Iowa City, IA) primary antibodies (1:1000 dilution), and goat anti-rabbit or mouse horseradish peroxidase-conjugated secondary antibodies (Zymed Laboratories; 1:5000). Bound antibodies were detected using an Immun-Star horseradish peroxidase chemiluminescent kit (Bio-Rad).

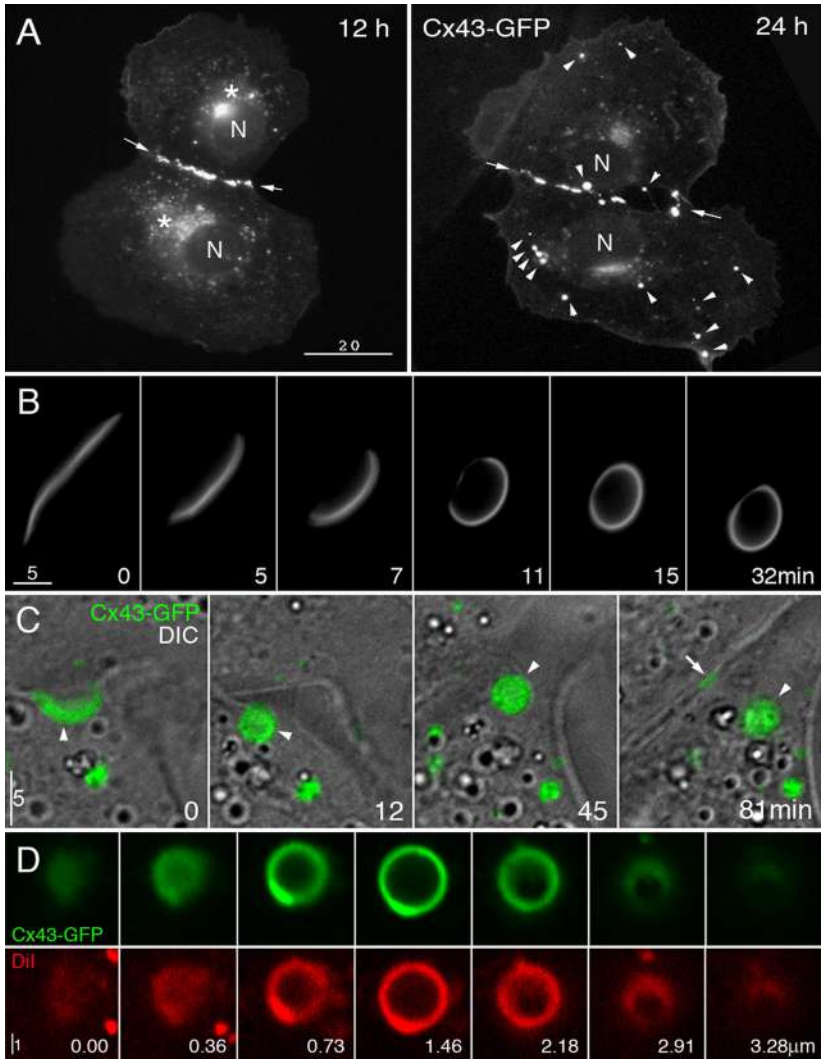

Figure 1. Internalization of GJs generates large cytoplasmic double-membrane vesicles. (A) Early after transfection (12 h), GJs assembled from Cx43-GFP are visible in the PM between transfected HeLa cells (labeled with arrows in all figures). In addition, secretory connexin cargo is visible in the Golgi region of the cell (labeled with asterisks). Later (24 h posttransfection) additional bright fluorescent vesicular structures (~1–5 μm in diameter) are detectable primarily in the cytoplasm of one cell (marked with arrowheads in all figures). (B) Time-lapse recording of a GJ plaque that internalizes to form such a double-membrane GJ vesicle, previously termed AGJs (also see Supplemental Movie 1B). (C) DIC and fluorescence time-lapse microscopy demonstrate the formation, detachment, and cytoplasmic translocation of AGJ vesicles away from the PM into the cell body. Note the assembly of a new GJ plaque in the membrane (labeled with an arrow; also see Supplemental Movie 1C). (D) Spherical membranous structure of AGJ vesicles revealed by DiI staining and confocal z-sectioning. (E) AGJ vesicles are double-membrane structures that are composed of connexons (GJ half-channels) derived from the PMs of both coupled cells. This was demonstrated by growing stably transfected Cx43-CFP (green) and Cx43-YFP (red) HeLa cells in mixed cultures. GJ plaques between red and green cells look yellow. Also, yellow internalized AGJ vesicles are detectable primarily in one of the two coupled cells. (F and G) The lumen of AGJ vesicles corresponds to cytoplasm derived from the neighboring cell. This was demonstrated by microinjecting one cell of a coupled pair with red fluorescent quantum dots (GJ impermeable). AGJ vesicles internalized into the labeled cell have a black lumen (F), whereas AGJ vesicles that bud into a noninjected cell have a red lumen (G). (H) Ultrastructural analysis of Cx43-GFP–transfected HeLa cells show all stages of progressive GJ internalization and AGJ vesicle formation. N, nuclei. Bars in all figures, micrometers in fluorescence and nanometers in electron microscopic images.

Statistical Analyses

Statistical analyses of AGJ dynamics and clathrin/myosin-VI involvement in GJ internalization was done by counting the number of Cx43-GFP–expressing cells, by counting the number of AGJ and GJ plaques, and by calculating the average number of GJ plaques and AGJs per cell using Microsoft Excel's analysis of variance (ANOVA) "Single Factor and Descriptive Statistics" functions of the data analysis package. In all analyses, a p value of <0.05 was considered significant. Data are expressed as mean ± SEM.

Online Supplemental Material

Online supplemental material consists of three video sequences to accompany Figures 1B, 1C, and 2A.

RESULTS

Entire GJ Plaques Internalize to Form Cytoplasmic GJ Vesicles

To investigate how GJs are degraded, HeLa cells were transfected with a GFP-tagged Cx43-expressing plasmid. Our comprehensive structural and functional analyses as well as those by others have shown that GFP-tagged Cxs assemble, traffic, and function comparably to untagged Cxs (Jordan *et al*., 1999; Bukauskas *et al*., 2000; Falk, 2000). Because HeLa cells do not express endogenous Cxs, all Cxs synthesized in the transfected cells were GFP tagged and visible. About 12 h posttransfection, GJ plaques were detectable in the PMs between contacting cells (marked with arrows in Figure 1A, left). In the Golgi region (marked with asterisks in Figure 1A, left), we also observed vesicular Cx43-GFP signal, which we have characterized previously as secretory Cx cargo destined for delivery to the PM (Lauf *et al*., 2002). At later time points (24–40 h posttransfection), the secretory Cx cargo signal was diminished. Instead, numerous bright, fluorescent puncta, ~1–5 μm in diameter, were detected in the cells' cytoplasm (Figure 1A, right, arrowheads). These puncta were asymmetrically distributed between the two coupled cells (72 ± 3% of puncta in one cell; 50 cells/575 puncta counted). Their fluorescence was as intense as the GJ plaques, suggesting that these puncta were internalized GJs. Subsequent live-cell imaging confirmed that entire GJ plaques, or large portions of plaques, were internalized to form GJ vesicles (Figure 1B and Supplemental Movie 1B). Combined fluorescence and differential interference contrast (DIC) imaging showed that internalized GJ vesicles, once formed, were completely detached from the PM and translocated into the cytoplasm (Figure 1C and Supplemental Movie 1C, arrowhead). Note the reappearance of a new GJ plaque in the PM (Figure 1C, rightmost panel, arrow). Internalization of GJ plaques occurred within 20–60 min (n = 10).

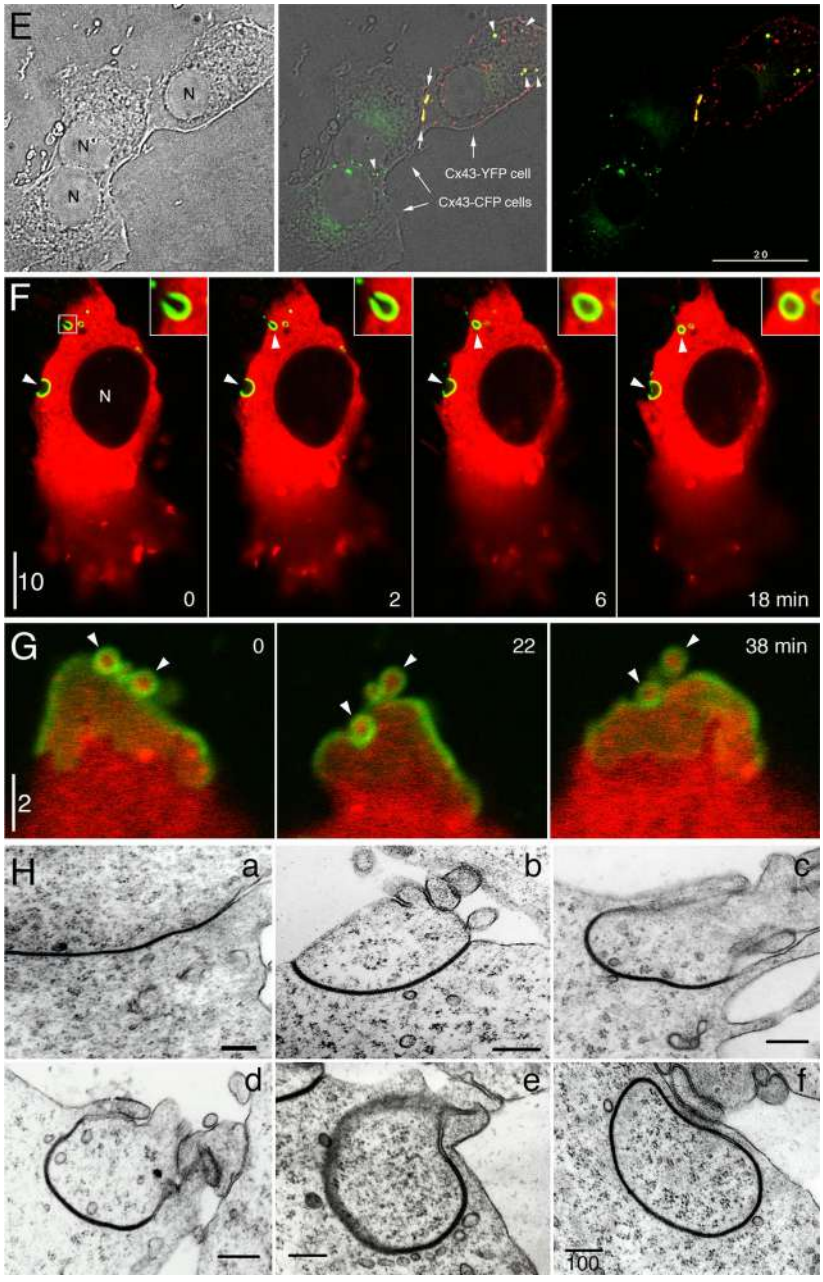

Figure 1 (cont).

To further characterize the structural organization of internalized GJs, additional analyses were performed. Confocal z-sectioning in the presence of the lipid stain DiI revealed the spherical structure and membranous nature of the internalized GJ vesicles (Figure 1D). To verify that these cytoplasmic GJ structures were indeed double-membrane vesicles containing connexons derived from both adjacent cell membranes, HeLa cells stably expressing Cx43-CFP and Cx43-YFP were generated and seeded in mixed cultures. GJs formed between Cx43-CFP–expressing cells (pseudocolored green in Figure 1E) and Cx43-YFP–expressing cells (pseudocolored red in Figure 1E) looked yellow, the resulting color of overlaying green and red fluorescence (Figure 1E, arrows). We also observed yellow-looking cytoplasmically located GJ vesicles, which were internalized with a directional bias into one cell of the cell pair (marked with arrowheads in Figure 1E). To demonstrate that the lumen of these GJ vesicles contained cytoplasm derived from the neighboring cell, one cell of a pair (coupled by Cx43-GFP-based GJs) was microinjected with red fluorescent quantum-dots (Qtracker 655; GJ impermeable) and followed by time-lapse imaging. GJ plaques that invaginated into the microinjected cells resulted in AGJ vesicles with a black lumen (Figure 1F, arrowheads), whereas GJs that budded into the noninjected cells resulted in AGJ vesicles with a red lumen (Figure 1G, arrowheads). Finally, ultrastructural analyses of thin-sectioned Cx43-GFP–expressing HeLa cells showed the electron-dense, striated staining typical for gap and annular junctions and revealed all stages of progressive GJ internalization described above (Figure 1H). In summary, our results demonstrate that entire GJs or large portions of GJs are internalized to form cytoplasmic AGJ vesicles.

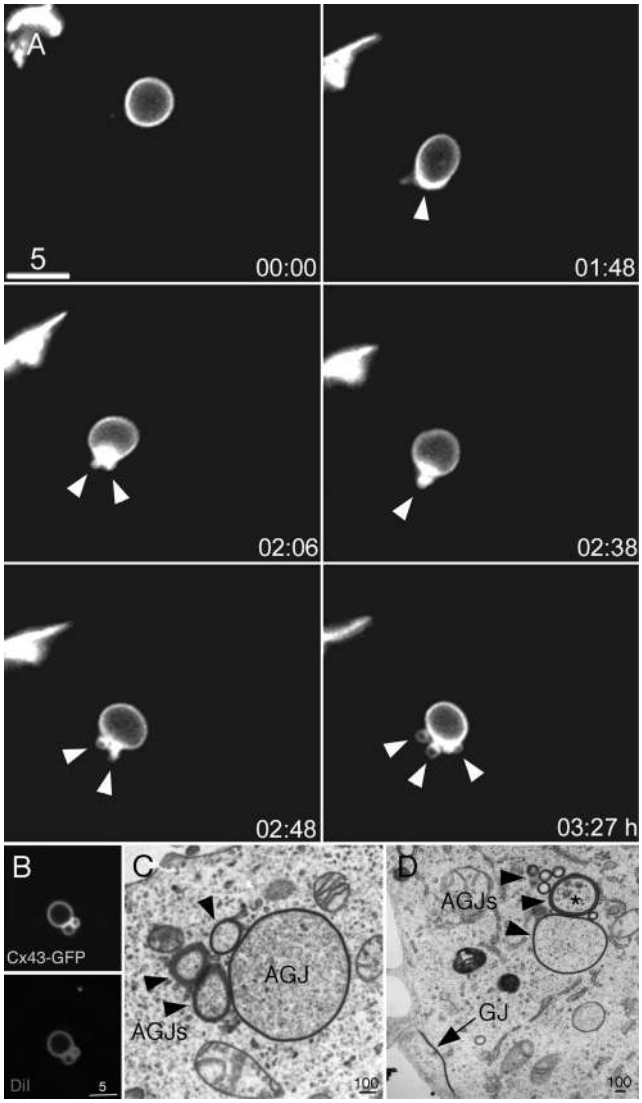

Figure 2. Internalized double-membrane GJ vesicles fragment into smaller vesicles. (A) Time-lapse recordings of Cx43-GFP–transfected HeLa cells demonstrate initial degradation of AGJ vesicles by successive budding of smaller AGJ vesicles from a newly internalized, larger AGJ vesicle (marked with arrowheads; also see Supplemental Movie 2A). (B) Confocal section of an AGJ vesicle cluster stained with DiI. (C and D) Ultrastructural composition of AGJ vesicles from Cx43-GFP–transfected HeLa cells. Note the "collapsed" AGJ vesicle with its two closely apposed double-membrane envelopes (D, asterisk).

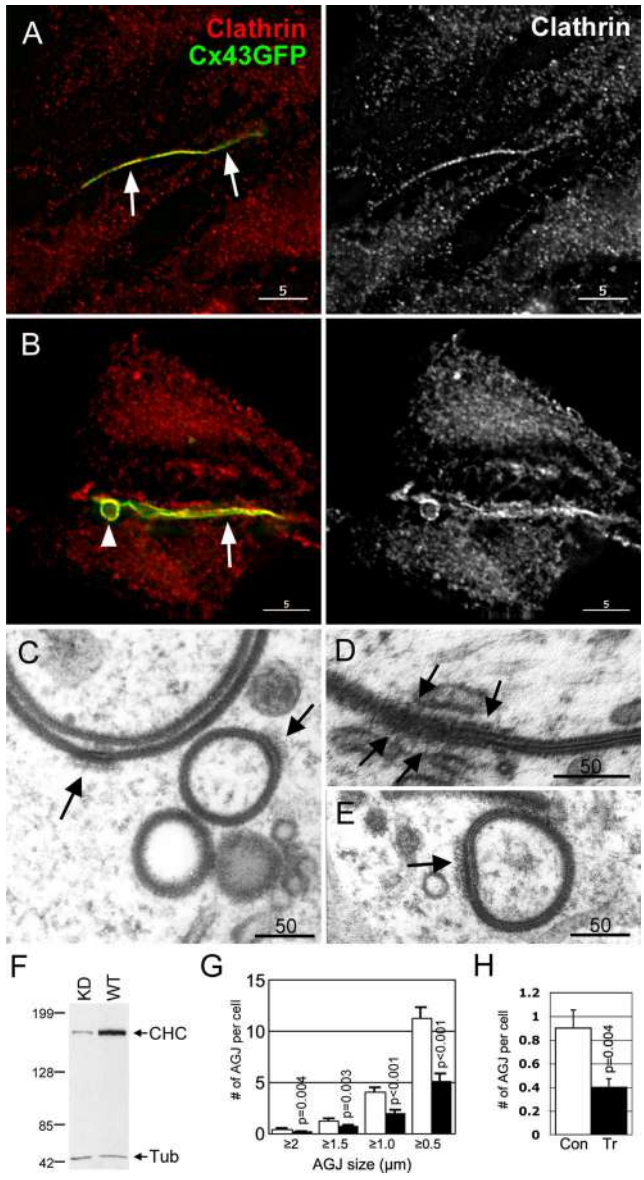

Figure 3. Double-membrane GJ internalization is clathrin mediated. (A and B) Colocalization of clathrin patches with GJs and internalized AGJ vesicles in Cx43-GFP–transfected HeLa cells. (C–E) Defined patches of dense protein coats with the characteristic thickness and appearance of clathrin coats on the outside of internalized GJ vesicles (C and E), and on GJ plaques (D). (F) Significant reduction of clathrin heavy chain (CHC) expression by RNAi (Tub, β-tubulin; WT, wild type). (G) Significant reduction of internalized GJ numbers in KD cells (number of cells = wt [157] and KD]189]; internalized GJ vesicles counted and grouped by size (wt [KD]): ≥2 μm: 68 [40]; ≥1.5 μm: 199 [134]; ≥1 μm: 645 [366]; and ≥0.5 μm 1759 [973]). Data shown are mean ± SEM. p values indicate significance. (H) Significant reduction ($p = 0.04$) of internalized GJ vesicle numbers in hypertonic medium treated cells (number of untreated cells, 125; number of treated cells, 99; Con, control cells; Tr, treated cells). Only AGJ vesicles ≥2 μm in diameter were counted. Data shown are mean ± SEM.

Subsequent to Internalization AGJ Vesicles Fragment into Smaller Vesicles Suitable for Degradation

We performed additional time-lapse imaging to investigate the fate of GJs after their internalization. Our observations showed that AGJ vesicles, after internalization and translocation, fragmented into smaller vesicles. Specifically, smaller AGJ vesicles were observed to bud from a specific initiation site on the surface of a larger AGJ vesicle (Figure 2A, arrowheads, and Supplemental Movie 2A). This resulted in a clear reduction of parent AGJ vesicle size (by ~2 μm in the example shown) and a cluster of closely apposed smaller and larger AGJ vesicles. Confocal analysis in the presence of DiI revealed the mixed lipid/Cx composition (Figure 2B), and electron microscopic examination revealed the ultrastructural composition of these AGJ vesicle clusters in the cytoplasm of the Cx43-GFP–transfected HeLa cells (Figure 2, C and D). Overall, these results demonstrate that GJs, after internalization and translocation into the cytoplasm, fragment into smaller AGJ vesicles suitable for further degradation shown to occur primarily via endo/lysosomal path-

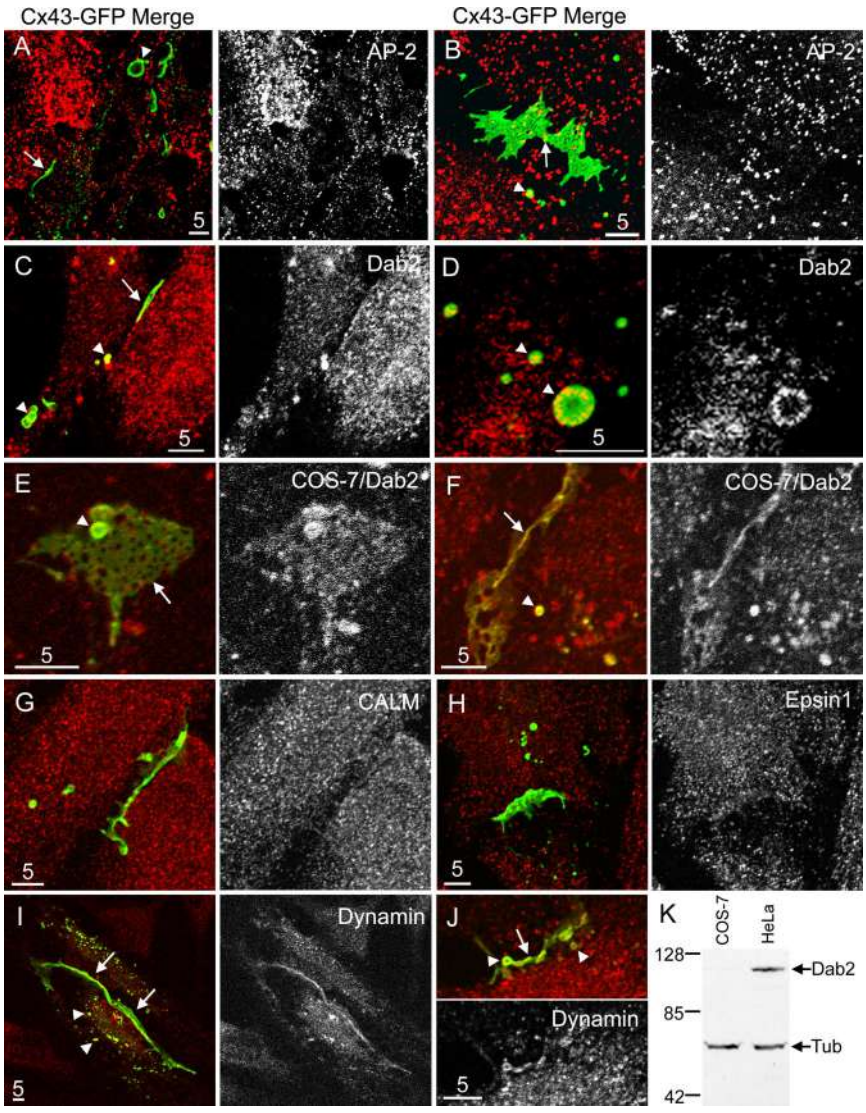

Figure 4. Colocalization of clathrin adaptors and dynamin with Cx43-based GJs and AGJ vesicles. GJs are marked with arrows. AGJ vesicles are marked with arrowheads. (A and B) The classical PM clathrin adaptor AP-2 shows minimal colocalization with GJs and AGJ vesicles. (C and D) The alternative potent clathrin adaptor Dab-2 colocalizes robustly with GJs and AGJ vesicles in Cx43-GFP–transfected HeLa cells. (E and F) Specificity of the Dab2/Cx43 colocalization was tested in COS-7 cells that express significantly lower levels of Dab2 (see immunoblot in K). Other known potent clathrin adaptor proteins CALM (G) or epsin1 (H) exhibited weak colocalization with Cx43-GFP based GJs and AGJ vesicles. Dynamin also colocalizes robustly with GJs and AGJ vesicles (I and J).

ways (Ginzberg and Gilula, 1979; Qin *et al*., 2003; Berthoud *et al*., 2004; Leithe *et al*., 2006; our unpublished data). Thus, smaller AGJ vesicles can be derived from processes other than internalization of small GJ plaques.

Clathrin Is Recruited to GJs and AGJ Vesicles and Is Required for GJ Internalization

In previous studies, a dense protein coat was detected on the outer surface of AGJs by ultrastructural analyses (Larsen *et al*., 1979). We thus investigated clathrin localization in our Cx43-GFP–expressing HeLa cells. A robust colocalization of clathrin recruited to defined patches was detectable along the surface of GJs (marked with arrows) as well as AGJ vesicles (marked with arrowheads) by confocal microscopy (Figure 3, A and B). The same patchy distribution was observed using different clathrin-specific monoclonal and polyclonal antibodies (directed against either clathrin heavy or light chains; see *Materials and Methods*), with untagged Cx43 expression, and with endogenous Cx43 in COS-7 cells (data not shown). Patches of dense protein with the characteristic thickness and appearance of clathrin coats were also detected on the outside of AGJ vesicles and on GJ plaques by ultrastructural analyses of our Cx43-GFP–expressing HeLa cells (Figure 3, C–E, arrows).

Because cells have developed several mechanistically distinct endocytic pathways (Conner and Schmid, 2003), we tested the importance of clathrin for the internalization of GJ plaques by depleting HeLa cells of clathrin-heavy chain by RNAi as determined by Western blot analyses (Figure 3F). Endocytosis inhibition was verified by fluorescent transferrin uptake, which was nearly abolished in the RNAi-treated cells (data not shown). AGJ vesicles were then counted in wild-type (wt) and knockdown (KD) Cx43-GFP–transfected cells. In three independent experiments, we found a significant reduction in the number of AGJ vesicles that were internalized in the clathrin KD cells (55%; Figure 3G). A similar result (56% reduction) was obtained when we cultivated Cx43-GFP–transfected HeLa cells in hypertonic medium, a treatment described to prevent clathrin and adaptor proteins from interacting (Heuser and Anderson, 1989; Hansen *et al*., 1993; Figure 3H). Overall, these investigations demonstrate a critical role for clathrin in the internalization and degradation of Cx43-based GJs.

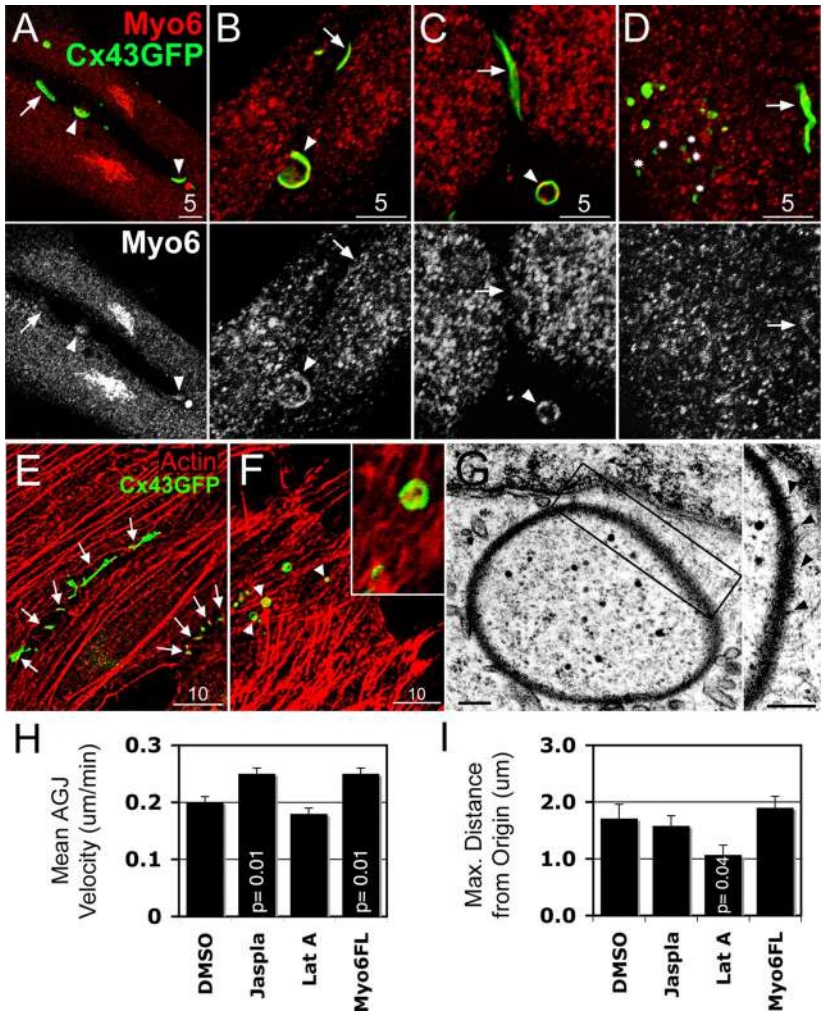

Figure 5. Myosin-VI colocalizes with invaginating plaques and AGJ vesicles, and actin/myosin-VI activity drives AGJ vesicle translocation. (A–D) Myosin-VI colocalizes specifically with internalizing GJ plaques and with newly internalized AGJ vesicles (marked with arrowheads) but not with planar GJs (marked with arrows), late AGJ vesicle degradation products, or Cx43-GFP–containing secretory cargo vesicles (marked with asterisks) as indicated by confocal colocalization studies of Cx43-GFP–transfected HeLa cells. (E–G) Actin filaments (stained with rhodamine-phalloidin in E and F) colocalize with GJs (E, arrows) and AGJ vesicles (F and G, arrowheads) in Cx43-GFP–transfected HeLa cells (confocal microscopy in E and F; ultrastructural analyses in G). To examine the involvement of actin/myosin-VI in AGJ vesicle translocation, actin filaments were either stabilized (by treating the cells with jasplakinolide [Jaspla]) or disrupted (by treating with latrunculin A [LatA]), or a GFP-tagged full length (Myo6FL) construct was coexpressed with Cx43-GFP and the mean velocity (H) and the maximum distance traveled (I) of AGJ vesicles was measured (number of cells [AGJ vesicles] tracked for DMSO: 7 [11]; jasplakinolide: 8 [21]; latrunculin A: 9 [20]; control cells: 20 [28]; and GFP-M6full–expressing cells: 22 [44]; ANOVA; $p < 0.05$).

The Alternative Clathrin-Adaptor Dab2 and the GTPase Dynamin Are Specifically Recruited to Cx43-based GJs and AGJ Vesicles

Clathrin does not interact directly with endocytic cargo, but it is typically recruited by interaction with the adaptor protein complex AP-2 that binds to the cargo receptor. Thus, we examined whether AP-2 colocalizes with Cx43-based GJs and AGJ vesicles. Surprisingly, a very weak colocalization (much less pronounced than the clathrin/GJ colocalization) was observed by confocal analyses (Figure 4, A and B). Recently, several alternative adaptor proteins have been described that interact with cargo-receptors and clathrin (Puertollano, 2004; Traub, 2005). Thus, we tested whether one of the other potent clathrin-binding adaptors, Disabled-2 (Dab2), CALM, or epsin, would colocalize with GJ and/or AGJ vesicles. We found that Dab2, but not CALM or epsin, efficiently localized to Cx43-based GJs, internalizing plaques, and AGJ vesicles in a similar pattern to clathrin (Figure 4, C–H). Because HeLa cells express relatively high levels of Dab2 (Figure 4K), we tested the significance of this colocalization in COS-7 cells, which are known to express low levels of Dab2 (Figure 4K; Dance *et al.*, 2004). Under these low Dab2 expression conditions, an equally robust colocalization between Cx43-GFP–based GJs, AGJ vesicles, and Dab2 was observed (Figure 4, E and F). Similar results were also obtained with untagged Cx43 expression and with endogenous Cx43 in COS-7 cells (data not shown).

Another protein that is recruited to clathrin-coated pits is the GTPase dynamin, which functions in the completion of vesicle budding (Conner and Schmid, 2003). Robust colocalization of dynamin with Cx43-based GJs and especially invaginating plaques and AGJ vesicles also was observed (Figure 4, I and J).

Myosin-VI Is Specifically Recruited to Invaginating GJs and Translocates Internalized GJ Vesicles along Actin Filaments into the Cytoplasm

Myosin-VI (myo6) is the only motor protein known to migrate toward the pointed (minus) ends (located peri-nuclearly) of actin filaments (Hasson and Mooseker, 1994). Recently, it has been described to function in translocating vesicles generated by clathrin-dependent endocytosis from the PM through the peripheral actin meshwork into the cell body (Aschenbrenner *et al.*, 2004; Dance *et al.*, 2004). myo6 can interact directly with Dab2 and thus can link cargo and endocytic vesicles to actin filaments (Morris *et al.*, 2002; Dance *et al.*, 2004). Because endocytic vesicles are generally much smaller (< 0.2 μm in diameter) than newly generated AGJ vesicles (often >0.5 μm in diameter), we wondered whether myosin-VI might also be involved in the translocation of AGJ vesicles.

Staining Cx43-GFP–transfected HeLa cells with anti-myosin-VI antibodies revealed a robust colocalization of myosin-VI specifically with internalizing plaques and newly

generated AGJ vesicles (Figure 5, A–C, arrowheads). Colocalization with planar GJ plaques (marked with arrows in Figure 5, A–D), fragmented AGJ vesicles (<0.5 μm in diameter), or with Cx43-GFP–containing secretory vesicles (Figure 5D, asterisks) was not observed. In addition to myosin-VI colocalization, we also observed colocalization of GFP-based GJs and AGJ vesicles with actin filaments stained with rhodamine-phalloidin (confocal microscopy; Figure 5, E and F, arrows). Actin filament/AGJ vesicle colocalization was confirmed by ultrastructural analyses (Figure 5G, arrowheads) and is consistent with reports from others using endogenously expressed Cxs (Larsen *et al.*, 1979).

Next, we investigated whether myosin-VI was involved in the translocation process of AGJ vesicles along actin filaments as suggested by the GJ/AGJ vesicle-myosin-VI–actin filament colocalization. Thus, we depolymerized or stabilized actin filaments or overexpressed a GFP-tagged myosin-VI fusion protein (GFP-M6full) in HeLa cells. Using time-lapse image sequences of Cx43-GFP–based AGJ vesicles in living HeLa cells, we determined AGJ vesicle dynamics and calculated the mean velocity and maximum distance AGJ vesicles traveled per unit time. When cells were treated with jasplakinolide (actin filament stabilizer), the mean AGJ vesicle velocity increased significantly (0.20 $\pm$ 0.01–0.25 $\pm$ 0.01 μm/min; $p = 0.01$; Figure 5H). Similarly, overexpression of full-length myosin-VI significantly increased mean AGJ vesicle velocity (0.20 $\pm$ 0.01–0.25 $\pm$ 0.01 μm/min; $p = 0.01$; Figure 5H). Alternatively, treatment with latrunculin A (actin filament depolymerizer) resulted in a significant decrease in AGJ vesicle mobility, as determined by calculating the maximum distance traveled from the point of origin (1.7 $\pm$ 0.3–1.1 $\pm$ 0.2 μm; $p = 0.04$; Figure 5I). Overall, our observed changes in AGJ vesicle mobility indicate that myosin-VI translocates AGJ vesicles away from the PM periphery deeper into the cytoplasm for subsequent degradation. The number of GJs and AGJ vesicles was unchanged in all these experiments (all p values >0.164), indicating no role for myosin-VI in earlier processes of GJ internalization.

We also investigated myosin-II, a conventional plus-end–directed actin-based motor previously suggested to colocalize with internalized AGJs (Murray *et al.*, 1997). Using myosin-IIA and myosin-IIB–specific anti-peptide antibodies, we found no localization of myosin-II to the membrane periphery of HeLa cells or to GJs, invaginating plaques, or newly formed AGJ vesicles (data not shown). Treating cells with blebbistatin, a myosin-II–specific inhibitor did not significantly alter the number of AGJ vesicles generated compared with cells that were treated with solvent (DMSO) only (50 cells treated with solvent, 555 AGJ vesicles in total, 11 $\pm$ 1 AGJ vesicles/cell; 50 cells treated with blebbistatin, 401 AGJ vesicles in total, 8 $\pm$ 2 AGJ vesicles/cell; $p = 0.2$; ANOVA), suggesting no involvement of myosin-II in GJ internalization.

DISCUSSION

Formation of Double-Membrane GJ Vesicles

Early ultrastructural analyses revealed large vesicular double-membrane GJ structures, AGJs, in the cytoplasm of cells derived from many different tissues (Ginzberg and Gilula, 1979; Larsen *et al.*, 1979; Pfeifer, 1980; Leach and Oliphant, 1984; Mazet *et al.*, 1985; Severs *et al.*, 1989). Here, we demonstrate by expressing Cx43-GFP (a major GJ subunit protein) in HeLa cells, that entire GJ plaques can be internalized into one of the coupled cells to form these cytoplasmic, double-membrane GJ vesicles (Figure 1). Our studies also show that nascent AGJ vesicles, subsequent to internalization, fragment into smaller AGJ vesicles (Figure 2) suitable for further degradation by endo/lysosomal pathways (Ginzberg and Gilula, 1979; Qin *et al.*, 2003; Berthoud *et al.*, 2004; Leithe *et al.*, 2006; our unpublished data). Internalization of entire GJs, as observed in our study is likely to have a profound impact on the coupling capacity of cells.

Because cell–cell coupling can be regulated by GJ channel gating (Delmar *et al.*, 2004; Lampe and Lau, 2004; Moreno, 2005), removal of GJ plaques from the membrane suggests that the gating function of channels may decrease/cease; or that Cx43 performs functions in addition to direct cell–cell coupling that requires relocation of Cx43 into the cytoplasm (Giepmans, 2004; Jiang and Gu, 2005). Finally, by internalizing entire GJ plaques, injured, infected, metastatic, apoptotic, or mitotic cells could uncouple permanently or transiently from neighboring cells. Notably, GFP-claudin-3–labeled tight junctions assembled in mouse Eph4 epithelial cells were recently shown to undergo an analogous internalization process with the two apposed membranes coendocytosed into one of the two adjacent cells (Matsuda *et al.*, 2004). Endocytosis of adherens junctions (AJs) after calcium depletion has also been reported to occur via a clathrin-mediated pathway; however, AJs are first separated symmetrically and components are internalized into both previously coupled cells (Ivanov *et al.*, 2004a,b). Desmosomes, another class of cell–cell junctions, also seem to be separated symmetrically into half-desmosomes before internalization, however, in a supposedly clathrin-independent mechanism (Holm *et al.*, 1993).

GJ channel turnover and internalization has been investigated previously by time-lapse microscopy. However, previous studies analyzed the assembly and turnover of channels within GJ plaques (Gaietta *et al.*, 2002; Lauf *et al.*, 2002), or only small fragments of GJ plaques were observed to internalize within seconds, or a few minutes (Jordan *et al.*, 2001; our unpublished data). Although the process of GJ channel removal from plaques remains unclear, published work indicates that channels within a plaque are turned over continuously. It is possible that this occurs in small portions and that this process has been captured in the Jordan *et al.* (2001) study. Here, in contrast, we describe the internalization of complete or large portions of GJ plaques, which occurred over a period of 20–60 min.

Proteins Involved in GJ Internalization

We found that the coat protein clathrin, the alternative adaptor protein Dab2, the GTPase dynamin, the unconventional myosin, myosin-VI, and actin filaments seem to be directly involved in the internalization, inward movement, and initial degradation of GJ channel plaques (Figures 3–5). Spatiotemporal analyses indicated where and when these protein components interact with GJs and AGJ vesicles (Table 1), and allowed us to generate a conceptual model for GJ internalization and degradation (Figure 6). Together, we show for the first time that a clathrin-dependent endocytic process internalizes double-membrane regions that can be 50 times larger than a typical endocytic vesicle (Conner and Schmid, 2003). In addition, this internalization process occurs on lateral membranes that contact neighboring cells. Recent consistent reports have shown clathrin-related internalization of large particles, such as viruses and pathogenic bacteria (Ehrlich *et al.*, 2004; Rust *et al.*, 2004; Veiga and Cossart, 2005) and of large latex beads (Aggeler and Werb, 1982).

In an early ultrastructural study, clathrin had been speculated to be involved in GJ internalization (Larsen *et al.*, 1979); however, a robust colocalization of clathrin with GJs,

Table 1. Spatiotemporal analysis of components colocalizing with Cx43-based GJ internalization and degradation intermediates

Colocalization	Planar GJ plaque	Invaginating GJ plaque	Early AGJ	Late AGJ
Clathrin heavy chain	+++	+++	+++	−
Clathrin light chain	+++	+++	+++	−
AP-2	+	+	+	−
Dab2	+++	+++	+++	−
PtdIns(4,5)P_2	−	−	−	−
CALM	−	−	−	−
Epsin	−	−	−	−
Dynamin	+	++	+++	−
Myosin-VI	−	++	+++	−
Myosin-IIA	−	−	−	na
Myosin-IIB	−	−	−	na
F-actin	++	++	++	+

+++, ++, +, and − represent strong, intermediate, weak, and no detectable colocalization, respectively. na, not analyzed.

internalizing plaques, and AGJ vesicles as described in our study had not been reported. The crucial role of clathrin for GJ internalization was demonstrated in our study by a significant reduction in AGJ vesicle formation in clathrin KD cells (Figure 3, F and G), and in cells cultivated in hypertonic medium (Figure 3H), a treatment known to prevent clathrin and adaptor proteins from interacting (Heuser and Anderson, 1989; Hansen *et al*., 1993). Unexpectedly, we found that clathrin did not seem to coat the entire surface of GJs and AGJ vesicles, but it was distributed in distinct patches (Figure 3, A–E). Clathrin patches have been detected on the cytoplasmic PM surface and clathrin triskelia can assemble into lattices with varying curvatures (Heuser and Anderson, 1989; Fotin *et al*., 2004). Together, these studies suggest that adaptable clathrin coats can accommodate the internalization of vesicles and other structures that vary significantly in size and shape.

Generally, clathrin interacts indirectly with endocytic cargo via the adaptor protein complex AP-2 that binds both the cargo receptor and clathrin (Traub, 2005). We did not observe significant colocalization of GJs and AGJ vesicles with AP-2; instead, we found a pronounced colocalization with the alternative clathrin adaptor disabled-2 (Dab2). The colocalization of Dab2 with Cx43-based GJs and AGJ vesicles seemed to be highly specific as indicated by an equivalently robust Dab2 staining of GJs and AGJ vesicles in COS-7 cells, which express low levels of Dab2 (Figure 4K) (Dance *et al*., 2004). Dab2 belongs to a new family of alternative clathrin adaptors (including β-arrestin, ARH, AP180/CALM, HIP1, epsin, and numb) that were found to interact with certain classes of cargo (Traub, 2003; Puertollano, 2004). Colocalization of Cx43-GFP–based GJs and AGJ vesicles with other potential potent clathrin-binding adaptors, including CALM and epsin 1, was not observed.

Dab2 has been found to be involved in the internalization of LDL-receptor family members by recognizing and binding to a tyrosine-based internalization motif of the type NPXY (N, asparagine; P, proline; X, any amino acid residue; and Y, tyrosine) via its N-terminal phosphotyrosine-binding (PTB) domain (Morris and Cooper, 2001; Mishra *et al*., 2002). In addition, Dab2 can bind directly to PtdIns(4,5)P_2 found in lipid membranes. Both reactions trigger clathrin triskelia assembly and cargo internalization via clathrin-coated vesicles (Morris and Cooper, 2001; Mishra *et al*., 2002; Hinrichsen *et al*., 2003; Motley *et al*., 2003; Mauer and Cooper, 2006). Using the PH domain of phospholipase C_δ linked to GFP as a fluorescent probe, we did not find a significant colocalization of PtdIns(4,5)P_2 with GJs (data not shown). Alternatively, conserved putative Dab2 binding motifs of the type XPXY are present in the C terminus of Cx43 ($P_{283}PGY_{286}$) and at least eight additional mouse and human Cxs (including hCx31.9 and its mouse orthologue mCx30.2, h/mCx32, h/mCx37, h/mCx45, h/mCx46, h/mCx47, h/mCx50, and hCx59), suggesting a potential direct interaction of Dab2 with a number of Cxs. Notably, mutation of critical amino acid residues within and around the putative Cx43-Dab2 binding site (P_{283}, Y_{286}, and V_{289}) significantly increased the half-life and the PM localization of Cx43 (Thomas *et al*., 2003), suggesting a pivotal role for Dab2 in GJ internalization.

In addition to its clathrin-adaptor function, Dab2 can associate via its C-terminal serine- and proline-rich region with the C-terminal globular tail of the minus-end–directed actin motor myo6. This association facilitates transport of

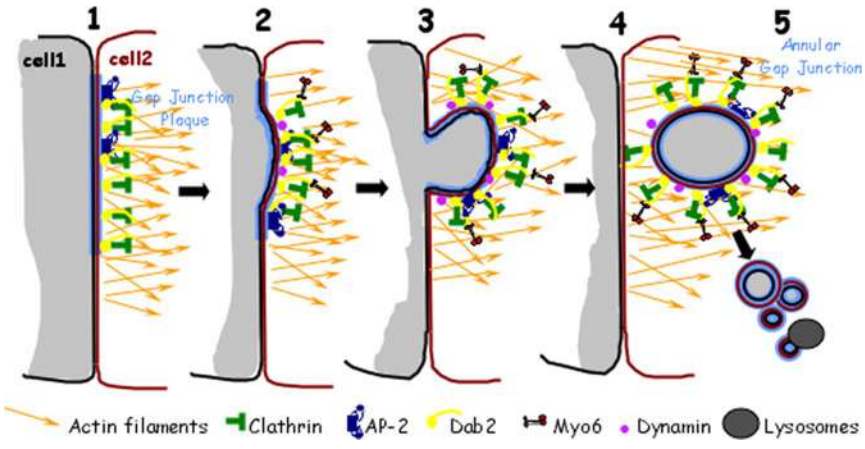

Figure 6. Schematic model of GJ internalization and degradation based on protein components that were characterized in this work. The alternative potent clathrin adaptor Dab2 is recruited to Cx43-based GJs possibly through a direct interaction of its N-terminal phosphotyrosine binding (PTB) domain with a putative XPXY internalization motif located in the C-terminal tail of Cx43 and in a number of other connexin family members. The distal portion of Dab2 on its opposite end binds the globular N-terminal domain of clathrin heavy chains and triggers clathrin lattice assembly. The GTPase dynamin is also recruited to GJs, resulting in double-membrane protrusion/invagination, neck restriction, and double-membrane scission. Other proteins, such as AP-2 or epsin might be recruited transiently, or in smaller numbers either actively or passively through their interaction with Cx43, Dab2, and/or clathrin. Dab2 then associates through its C-terminal serine- and proline-rich region with the C-terminal globular tail of myosin-VI that binds through its N-terminal motor domain to actin filaments resulting in the inward translocation of the internalized double-membrane GJ vesicles. GJ vesicles then fragment into smaller vesicles that are degraded by endo/lysosomal pathways.

nascent endocytic vesicles from the PM toward the cell interior (Morris *et al*., 2002; Aschenbrenner *et al*., 2003, 2004; Hasson, 2003; Dance *et al*., 2004). We observed a robust recruitment of myosin-VI specifically to internalizing Cx43-based GJs and AGJ vesicles but not to planar GJ plaques (Figure 5, A–D). We also found actin filaments localized to GJs and AGJ vesicles in Cx43-GFP–transfected HeLa cells by structural and ultrastructural analyses (Figure 5, E–G), consistent with the well documented role of actin in GJ stabilization and internalization (Larsen *et al*., 1979; Naus *et al*., 1993; Murray *et al*., 1997; Butkevich *et al*., 2004). Myosin-VI–driven translocation of AGJ vesicles into the cytoplasm was indicated by the effect of stabilization of actin filaments or myosin-VI overexpression on AGJ vesicle mean velocity (Figure 5H). Additionally, disruption of actin filaments significantly reduced AGJ vesicle mobility (Figure 5I).

Comparable Clathrin-mediated Internalization Processes

Internalization of double-membrane GJ vesicles is an intriguing process with similarities to phagocytosis or intracellular pathogen (protozoa, bacteria, or viruses) invasion and cell-to-cell spreading (Johnson and Huber, 2002; Cossart *et al*., 2003; Gruenheid and Finlay, 2003; Rust *et al*., 2004; Gouin *et al*., 2005). AGJ vesicle formation requires active double-membrane protrusion and/or invagination, neck restriction, and double-membrane fission/resealing. How GJ protrusion/invagination is initiated is currently not known; however, GJs are internalized primarily into one of two coupled cells, indicating a highly regulated process. Actin polymerization has been linked to clathrin-dependent endocytosis, membrane protrusion, and invagination events as well as to the clathrin-mediated uptake of viruses and bacteria into host cells (Bonifacino and Glick, 2004; Ehrlich *et al*., 2004; Merrifield, 2004; Rust *et al*., 2004; Gouin *et al*., 2005; Veiga and Cossart, 2005; Yarar *et al*., 2005), suggesting that actin polymerization might also be involved in the internalization of GJs. The mechanism for double-membrane fission also remains unclear. Comparable events of mitochondrial outer and inner membrane fission and fusion occur in succession (Meeusen *et al*., 2004), suggesting that during GJ vesicle formation the two PMs are also separated successively. A striking similarity between a recent *Listeria* uptake study (Veiga and Cossart, 2005) and our GJ internalization study is that the clathrin-dependent endocytic machinery is used in both processes to internalize large structures without recruitment of the classical PM clathrin adaptor AP-2. To date, no clathrin-adaptor has been implicated in bacteria or virus internalization; however, based on our results, it is tempting to speculate that Dab-2 might enable/regulate the clathrin-mediated internalization of large structures. Whether myosin-VI is involved in the uptake/translocation of bacteria or viruses is also not known.

We also found a pronounced colocalization of dynamin with GJs and AGJ vesicles (Figure 4, I and J), suggesting that GJ internalization requires dynamin to release the invaginating GJ vesicle from the PM. This is not surprising, because dynamin has been shown to be involved in the majority of endocytic processes, including phagocytosis, caveolae- and clathrin-mediated endocytosis as well as the cellular entry of *Listeria* (Gold *et al*., 1999; Pelkmans *et al*., 2002; Conner and Schmid, 2003; Veiga and Cossart, 2005). Dynamin is known to be recruited to clathrin-coated pits, and evidence suggests that both actin polymerization and dynamin contribute to the formation, fission, and mobility of clathrin-coated vesicles (Conner and Schmid, 2003; Bonifacino and Glick, 2004; Merrifield, 2004; Yarar *et al*., 2005). Our discovery that several key-components of the clathrin-dependent endocytic machinery are involved in the generation of large, double-membrane vesicular structures adds exciting complexity to the dynamic field of endocytosis.

ACKNOWLEDGMENTS

We thank Tama Hasson, Linton Traub, Sandra Schmid, and Lynne Cassimeris for kindly providing antibodies, reagents, and special equipment; and Shu-Chih Chen (Northwest Hospital, Bothell, WA) for generating stable tet-on–inducible Cx43-CFP and Cx43-YFP HeLa cell lines. We also thank Falk laboratory members for valuable discussions, and Lynne Cassimeris, Kathy Iovine, and Linton Traub for critically reading the manuscript. Work in the Falk laboratory is supported by National Institutes of Health, National Institute of General Medical Sciences Grant GM-55725 and the Bioengineering and Bioscience 2020 Funds.

REFERENCES

Aggeler, J., and Werb, Z. (1982). Initial events during phagocytosis by macrophages viewed from outside and inside the cell: membrane-particle interactions and clathrin. J. Cell Biol. *94*, 613–623.

Aschenbrenner, L., Lee, T., and Hasson, T. (2003). Myo6 facilitates the translocation of endocytic vesicles from cell peripheries. Mol. Biol. Cell *14*, 2728–2743.

Aschenbrenner, L., Naccache, S. N., and Hasson, T. (2004). Uncoated endocytic vesicles require the unconventional myosin, Myo6, for rapid transport through actin barriers. Mol. Biol. Cell *15*, 2253–2263.

Beardslee, M. A., Laing, J. G., Beyer, E. C., and Saffitz, J. E. (1998). Rapid turnover of connexin43 in the adult rat heart. Circ. Res. *83*, 629–635.

Berthoud, V. M., Minogue, P. J., Laing, J. G., and Beyer, E. C. (2004). Pathways for degradation of connexins and gap junctions. Cardiovasc. Res. *62*, 256–267.

Bonifacino, J. S., and Glick, B. S. (2004). The mechanisms of vesicle budding and fusion. Cell *116*, 153–166.

Bruzzone, R., White, T. W., and Paul, D. L. (1996). Connections with connexins: the molecular basis of direct intercellular signaling. Eur. J. Biochem. *238*, 1–27.

Bukauskas, F. F., Jordan, K., Bukauskiene, A., Bennett, M. V., Lampe, P. D., Laird, D. W., and Verselis, V. K. (2000). Clustering of connexin 43-enhanced green fluorescent protein gap junction channels and functional coupling in living cells. Proc. Natl. Acad. Sci. USA *97*, 2556–2561.

Butkevich, E., Hulsmann, S., Wenzel, D., Shirao, T., Duden, R., and Majoul, I. (2004). Drebrin is a novel connexin-43 binding partner that links gap junctions to the submembrane cytoskeleton. Curr. Biol. *14*, 650–658.

Chin, D. J., Straubinger, R. M., Acton, S., Nèathke, I., and Brodsky, F. M. (1989). 100-kDa polypeptides in peripheral clathrin-coated vesicles are required for receptor-mediated endocytosis. Proc. Natl. Acad. Sci. USA *86*, 9289–9293.

Conner, S. D., and Schmid, S. L. (2003). Regulated portals of entry into the cell. Nature *422*, 37–44.

Cossart, P., Pizarro-Cerda, J., and Lecuit, M. (2003). Invasion of mammalian cells by *Listeria* monocytogenes: functional mimicry to subvert cellular functions. Trends Cell Biol. *13*, 23–31.

Dance, A. L., Miller, M., Seragaki, S., Aryal, P., White, B., Aschenbrenner, L., and Hasson, T. (2004). Regulation of myosin-VI targeting to endocytic compartments. Traffic *5*, 798–813.

Delmar, M., Coombs, W., Sorgen, P., Duffy, H. S., and Taffet, S. M. (2004). Structural bases for the chemical regulation of Connexin43 channels. Cardiovasc. Res. *62*, 268–275.

Ehrlich, M., Boll, W., Van Oijen, A., Hariharan, R., Chandran, K., Nibert, M. L., and Kirchhausen, T. (2004). Endocytosis by random initiation and stabilization of clathrin-coated pits. Cell *118*, 591–605.

Falk, M. M. (2000). Connexin-specific distribution within gap junctions revealed in living cells. J. Cell Sci. *113*, 4109–4120.

Fallon, R. F., and Goodenough, D. A. (1981). Five-hour half-life of mouse liver gap-junction protein. J. Cell Biol. *90*, 521–526.

Fotin, A., Cheng, Y., Sliz, P., Grigorieff, N., Harrison, S. C., Kirchhausen, T., and Walz, T. (2004). Molecular model for a complete clathrin lattice from electron cryomicroscopy. Nature *432*, 573–579.

Gaietta, G., Deerinck, T. J., Adams, S. R., Bouwer, J., Tour, O., Laird, D. W., Sosinsky, G. E., Tsien, R. Y., and Ellisman, M. H. (2002). Multicolor and electron microscopic imaging of connexin trafficking. Science *296*, 503–507.

Ghoshroy, S., Goodenough, D. A., and Sosinsky, G. E. (1995). Preparation, characterization, and structure of half gap junctional layers split with urea and EGTA. J. Membr. Biol. *146*, 15–28.

Giepmans, B. N. (2004). Gap junctions and connexin-interacting proteins. Cardiovasc. Res. *62*, 233–245.

Ginzberg, R. D., and Gilula, N. B. (1979). Modulation of cell junctions during differentiation of the chicken otocyst sensory epithelium. Dev. Biol. *68*, 110–129.

Gold, E. S., Underhill, D. M., Morrissette, N. S., Guo, J., McNiven, M. A., and Aderem, A. (1999). Dynamin 2 is required for phagocytosis in macrophages. J. Exp. Med. *190*, 1849–1856.

Goodenough, D. A., and Gilula, N. B. (1974). The splitting of hepatocyte gap junctions and zonulae occludentes with hypertonic disaccharides. J. Cell Biol. *61*, 575–590.

Gouin, E., Welch, M. D., and Cossart, P. (2005). Actin-based motility of intracellular pathogens. Curr. Opin. Microbiol. *8*, 35–45.

Gruenheid, S., and Finlay, B. B. (2003). Microbial pathogenesis and cytoskeletal function. Nature *422*, 775–781.

Hansen, S. H., Sandvig, K., and van Deurs, B. (1993). Clathrin and HA2 adaptors: effects of potassium depletion, hypertonic medium, and cytosol acidification. J. Cell Biol. *121*, 61–72.

Hasson, T. (2003). Myosin VI: two distinct roles in endocytosis. J. Cell Sci. *116*, 3453–3461.

Hasson, T., and Mooseker, M. S. (1994). Porcine myosin-VI: characterization of a new mammalian unconventional myosin. J. Cell Biol. *127*, 425–440.

Heuser, J. E., and Anderson, R. G. (1989). Hypertonic media inhibit receptor-mediated endocytosis by blocking clathrin-coated pit formation. J. Cell Biol. *108*, 389–400.

Hinrichsen, L., Harborth, J., Andrees, L., Weber, K., and Ungewickell, E. J. (2003). Effect of clathrin heavy chain- and α-adaptin-specific small inhibitory RNAs on endocytic accessory proteins and receptor trafficking in HeLa cells. J. Biol. Chem. *278*, 45160–45170.

Holm, P. K., Hansen, S. H., Sandvig, K., and van Deurs, B. (1993). Endocytosis of desmosomal plaques depends on intact actin filaments and leads to a nondegradative compartment. Eur. J. Cell Biol. *62*, 362–371.

Ivanov, A. I., McCall, I. C., Parkos, C. A., and Nusrat, A. (2004a). Role for actin filament turnover and a myosin II motor in cytoskeleton-driven disassembly of the epithelial apical junctional complex. Mol. Biol. Cell *15*, 2639–2651.

Ivanov, A. I., Nusrat, A., and Parkos, C. A. (2004b). Endocytosis of epithelial apical junctional proteins by a clathrin-mediated pathway into a unique storage compartment. Mol. Biol. Cell *15*, 176–188.

Jiang, J. X., and Gu, S. (2005). Gap junction- and hemichannel-independent actions of connexins. Biochim. Biophys. Acta *1711*, 208–214.

Johnson, D. C., and Huber, M. T. (2002). Directed egress of animal viruses promotes cell-to-cell spread. J. Virol. *76*, 1–8.

Jordan, K., Chodock, R., Hand, A. R., and Laird, D. W. (2001). The origin of annular junctions: a mechanism of gap junction internalization. J. Cell Sci. *114*, 763–773.

Jordan, K., Solan, J. L., Dominguez, M., Sia, M., Hand, A., Lampe, P. D., and Laird, D. W. (1999). Trafficking, assembly, and function of a connexin43-green fluorescent protein chimera in live mammalian cells. Mol. Biol. Cell *10*, 2033–2050.

Kumar, N. M., and Gilula, N. B. (1996). The gap junction communication channel. Cell *84*, 381–388.

Lampe, P. D., and Lau, A. F. (2004). The effects of connexin phosphorylation on gap junctional communication. Int. J. Biochem. Cell Biol. *36*, 1171–1186.

Larsen, W. J., Tung, H. N., Murray, S. A., and Swenson, C. A. (1979). Evidence for the participation of actin microfilaments and bristle coats in the internalization of gap junction membrane. J. Cell Biol. *83*, 576–587.

Lauf, U., Giepmans, B. N., Lopez, P., Braconnot, S., Chen, S. C., and Falk, M. M. (2002). Dynamic trafficking and delivery of connexons to the plasma membrane and accretion to gap junctions in living cells. Proc. Natl. Acad. Sci. USA *99*, 10446–10451.

Leach, D. H., and Oliphant, L. W. (1984). Degradation of annular gap junctions of the equine hoof wall. Acta Anat. *120*, 214–219.

Leithe, E., Brech, A., and Rivedal, E. (2006). Endocytic processing of connexin43 gap junctions: a morphological study. Biochem. J. *393*, 59–67.

Matsuda, M., Kubo, A., Furuse, M., and Tsukita, S. (2004). A peculiar internalization of claudins, tight junction-specific adhesion molecules, during the intercellular movement of epithelial cells. J. Cell Sci. *117*, 1247–1257.

Mauer, M. E., and Cooper, J. A. (2006). The adaptor protein Dab2 sorts LDL receptors into coated pits independently of AP-2 and ARH. J. Cell Sci. *119*, 4235–4246.

Mazet, F., Wittenberg, B. A., and Spray, D. C. (1985). Fate of intercellular junctions in isolated adult rat cardiac cells. Circ. Res. *56*, 195–204.

Meeusen, S., McCaffery, J. M., and Nunnari, J. (2004). Mitochondrial fusion intermediates revealed in vitro. Science *305*, 1747–1752.

Merrifield, C. J. (2004). Seeing is believing: imaging actin dynamics at single sites of endocytosis. Trends Cell Biol. *14*, 352–358.

Mishra, S. K., Keyel, P. A., Hawryluk, M. J., Agostinelli, N. R., Watkins, S. C., and Traub, L. M. (2002). Disabled-2 exhibits the properties of a cargo-selective endocytic clathrin adaptor. EMBO J. *21*, 4915–4926.

Moreno, A. P. (2005). Connexin phosphorylation as a regulatory event linked to channel gating. Biochim. Biophys. Acta *1711*, 164–171.

Morris, S. M., Arden, S. D., Roberts, R. C., Kendrick-Jones, J., Cooper, J. A., Luzio, J. P., and Buss, F. (2002). Myosin VI binds to and localises with Dab2, potentially linking receptor-mediated endocytosis and the actin cytoskeleton. Traffic *3*, 331–341.

Morris, S. M., and Cooper, J. A. (2001). Disabled-2 colocalizes with the LDLR in clathrin-coated pits and interacts with AP-2. Traffic *2*, 111–123.

Motley, A., Bright, N. A., Seaman, M. N., and Robinson, M. S. (2003). Clathrin-mediated endocytosis in AP-2-depleted cells. J. Cell Biol. *162*, 909–918.

Murray, S. A., Williams, S. Y., Dillard, C. Y., Narayanan, S. K., and McCauley, J. (1997). Relationship of cytoskeletal filaments to annular gap junction expression in human adrenal cortical tumor cells in culture. Exp. Cell Res. *234*, 398–404.

Naus, C. C., Hearn, S., Zhu, D., Nicholson, B. J., and Shivers, R. R. (1993). Ultrastructural analysis of gap junctions in C6 glioma cells transfected with connexin43 cDNA. Exp. Cell Res. *206*, 72–84.

Pelkmans, L., Pèuntener, D., and Helenius, A. (2002). Local actin polymerization and dynamin recruitment in SV40-induced internalization of caveolae. Science *296*, 535–539.

Pfeifer, U. (1980). Autophagic sequestration of internalized gap junctions in rat liver. Eur. J. Cell Biol. *21*, 244–246.

Piehl, M., and Cassimeris, L. (2003). Organization and dynamics of growing microtubule plus ends during early mitosis. Mol. Biol. Cell *14*, 916–925.

Puertollano, R. (2004). Clathrin-mediated transport: assembly required. Workshop on Molecular Mechanisms of Vesicle Selectivity. EMBO Rep. *5*, 942–946.

Qin, H., Shao, Q., Igdoura, S. A., Alaoui-Jamali, M. A., and Laird, D. W. (2003). Lysosomal and proteasomal degradation play distinct roles in the life cycle of Cx43 in gap junctional intercellular communication-deficient and -competent breast tumor cells. J. Biol. Chem. *278*, 30005–30014.

Rust, M. J., Lakadamyali, M., Zhang, F., and Zhuang, X. (2004). Assembly of endocytic machinery around individual influenza viruses during viral entry. Nat. Struct. Mol. Biol. *11*, 567–573.

Severs, N. J., Rothery, S., Dupont, E., Coppen, S. R., Yeh, H. I., Ko, Y. S., Matsushita, T., Kaba, R., and Halliday, D. (2001). Immunocytochemical analysis of connexin expression in the healthy and diseased cardiovascular system. Microsc. Res. Tech. *52*, 301–322.

Severs, N. J., Shovel, K. S., Slade, A. M., Powell, T., Twist, V. W., and Green, C. R. (1989). Fate of gap junctions in isolated adult mammalian cardiomyocytes. Circ. Res. *65*, 22–42.

Thomas, M. A., Zosso, N., Scerri, I., Demaurex, N., Chanson, M., and Staub, O. (2003). A tyrosine-based sorting signal is involved in connexin43 stability and gap junction turnover. J. Cell Sci. *116*, 2213–2222.

Traub, L. M. (2003). Sorting it out: AP-2 and alternate clathrin adaptors in endocytic cargo selection. J. Cell Biol. *163*, 203–208.

Traub, L. M. (2005). Common principles in clathrin-mediated sorting at the Golgi and the plasma membrane. Biochim. Biophys. Acta *1744*, 415–437.

Varnai, P., and Balla, T. (1998). Visualization of phosphoinositides that bind pleckstrin homology domains: calcium- and agonist-induced dynamic changes and relationship to myo-[3H]inositol-labeled phosphoinositide pools. J. Cell Biol. *143*, 501–510.

Veiga, E., and Cossart, P. (2005). *Listeria* hijacks the clathrin-dependent endocytic machinery to invade mammalian cells. Nat. Cell Biol. *7*, 894–900.

Yarar, D., Waterman-Storer, C. M., and Schmid, S. L. (2005). A dynamic actin cytoskeleton functions at multiple stages of clathrin-mediated endocytosis. Mol. Biol. Cell *16*, 964–975.